16

Direction of Arrival Estimation using the PRIME Algorithm

H.K. Hwang and Zekeriya Aliyazicioglu
California State Polytechnic University, Pomona
CA, USA

1. Introduction

Instead of using a single sensor, an array processing system (Allen & Ghavami, 2005 and Trees, 2002) with innovative signal processing can enhance the resolution of signal parameters. An array sensor system has multiple sensors distributed in space. This array configuration provides spatial samplings of the received waveform. A sensor array has better performance than the single sensor in signal reception and parameter estimation. It also has the ability to identify multiple targets.

Array processing systems are used in a wide range of applications such as radar, sonar, seismology, mobile communications, and medical diagnostics (Forsythe, 1997, Leeet et al., 2005, Xu et al., 2001, Hwang & Grados, 2008, Aliyazicioglu & Hwang, 2008). For example, in defense applications, it is important to identify the direction of a possible threat. One example of a commercial application is to identify the direction of an emergency cell phone call in order to dispatch a rescue team to the proper location. Accurate estimation of a signal direction of arrival (DOA) has received a tremendous interest in communication and radar systems of commercial and military applications in the past decades.

This chapter describes the estimation of signal parameters such as signal frequency or DOA using an array processing systems and advanced signal processing algorithms. This chapter concentrates on the discussion of the *P*olynomial *R*oot *I*ntersection for *M*ulti-Dimensional *E*stimation (PRIME) algorithm (Hatke & Keith, 1994). Processing the received data by PRIME algorithm requires array processor. The PRIME algorithm can be considered the extension of the *Mu*ltiple *Si*gnals *C*lassification (MUSIC) (Schmidt, 1986) and Root MUSIC algorithms (Ren & William, 1997), which are based on the Eigen-analysis method.

To estimate the frequency of the sinusoid or the DOA of a narrowband signal using the conventional method suffers resolution limitation. For example, frequency resolution Δf using N point Fast Fourier Transform (FFT) is $\Delta f = 1/NT$, where T is the sampling period. Improved frequency resolution using FFT would require a large number of data samples. In many real time applications, using a large sample data is not always feasible. If there are multiple sinusoids with a frequency spacing less than Δf, FFT won't be able to resolve them.

The angle resolution of a conventional antenna is limited by the antenna mainlobe beamwidth. The mainlobe beamwidth is proportional to the signal wavelength and inversely proportional to the physical size of the antenna. Improving angle resolution by using large aperture antenna or operating at higher frequency is not always a viable solution. Certain systems such as aircraft antennas or missile seekers have physical size limitations; they cannot accommodate large aperture antennas. Higher frequency usually has a larger amount of atmospheric absorption; it may limit the detection range.

Rather than improve the DOA of frequency resolution by hardware improvement, an array processor together with an advanced signal processing algorithm provides an innovative solution that improves the resolution of parameter estimation. This chapter provides a brief review of the PRIME algorithm and its application in estimating a signal DOA.

Since the PRIME algorithm is closely related to MUSIC and root MUSIC, section 2 provides a brief review of the MUSIC algorithm. Computer simulations are used to demonstrate the enhanced resolution of MUSIC in temporal and spatial processing applications. The effects of estimation accuracy as a function of signal to noise ratio (SNR), and correlation matrix estimation based on different temporal averaging, are also discussed. Section 3 discusses the root MUSIC algorithm. Basic equations for frequency and angle estimations are derived. Some simulation examples demonstrate how to estimate signal parameters without having to use a scan vector. Finally, the extension of the root MUSIC to PRIME equivalent to estimate multiple parameters is discussed in section 4. Estimation of a signal DOA (elevation and azimuth angles) is used as a demonstration example. Estimation of two independent parameters requires two independent equations. These are derived from a subset and full array approaches and their simulation examples are discussed in section 4.

2. The MUSIC Algorithm

*Mu*ltiple *Si*gnals *C*lassification (MUSIC) is one of the most commonly applied eigen-analysis methods. It works quite well both in frequency estimation or signal direction of arrival (DOA) estimation.

Consider the received data sequence u(n) consisting of L independent sinusoids in the white noise environment. The received data u(n) is expressed in Equation 2.1

$$u(n) = \sum_{k=1}^{L} A_k e^{j(2\pi f_k n + \theta_k)} + w(n), \; n = 1, 2, \ldots, N \tag{2.1}$$

where A_k, f_k, θ_k are the amplitude, frequency and phase of k independent sinusoids and w(n) is the white noise sequence.

Define the received data vector $\mathbf{u}$ as $\mathbf{u} = [u(1), u(2), \ldots, u(N)]^T$, then the data vector correlation matrix $\mathbf{R}$ is $\mathbf{R} = E[\mathbf{u}\mathbf{u}^H]$, where the superscript H represents the matrix complex conjugate transpose (Hermitian). Using the relationship of Equation (2.1) and independent noise assumption, matrix $\mathbf{R}$ can be expressed as Equation (2.2).

$$\mathbf{R} = \mathbf{SPS}^{H} + \sigma_w^2 \mathbf{I} \tag{2.2}$$

where $\mathbf{P} = \text{diag}[A_1^2, A_2^2, \ldots, A_L^2]$, $\mathbf{S} = \begin{bmatrix} e^{j2\pi f_1} & e^{j2\pi f_2} & \cdots & e^{j2\pi f_L} \\ e^{j2\pi 2f_1} & e^{j2\pi 2f_2} & \cdots & e^{j2\pi 2f_L} \\ \vdots & \vdots & \ddots & \vdots \\ e^{j2\pi Nf_1} & e^{j2\pi Nf_2} & \cdots & e^{j2\pi Nf_L} \end{bmatrix}$ and σ_w^2 is the noise variance and $\mathbf{I}$ is the identity matrix.

Let $\lambda_1, \lambda_2, \ldots, \lambda_N$, are the eigenvalues of the correlation matrix $\mathbf{R}$ and $\lambda_1 \geq \lambda_2 \geq \ldots \geq \lambda_N$, their associate eigenvectors are $\mathbf{q}_1, \mathbf{q}_2, \ldots, \mathbf{q}_N$ respectively.

If there are L independent signals, then eigenvectors $\mathbf{q}_1, \mathbf{q}_2, \ldots, \mathbf{q}_L$ span over the signal and noise subspace and eigenvectors $\mathbf{q}_{L+1}, \mathbf{q}_{L+2}, \ldots, \mathbf{q}_N$ span over the noise only subspace. Signal and noise subspace and noise only subspace are mutually orthogonal.

For frequency estimation, the MUSIC spectrum is computed according to Equation (2.3).

$$S_{MUSIC}(f) = \frac{1}{\mathbf{s}^H(f)\mathbf{V}_N\mathbf{V}_N^H\mathbf{s}(f)} \tag{2.3}$$

where $\mathbf{V}_N = [\mathbf{q}_{L+1}, \mathbf{q}_{L+2}, \ldots, \mathbf{q}_N]$, and $\mathbf{s}(f) = [1, e^{j2\pi f}, \ldots, e^{j2\pi(N-1)f}]^T$ is a scan vector that scans over all possible frequencies. If the scan frequency happens to be equal to one of the signal frequencies, then the scan vector is orthogonal to column space of $\mathbf{V}_N$. Thus the dominate peaks of $S_{MUSIC}(f)$ correspond to the L number of signals and frequencies.

The following example demonstrates the enhanced frequency resolution of the MUSIC algorithm.

Suppose there are 32 received data samples u(n), u(1), n = 0, 1, . . ., 31, where data sample u(n) consists of two equal amplitude sinusoids with normalized frequencies 0.115 and 0.135, and white noise. The signal to noise ratio = 10 dB.

$$u(n) = e^{j2\pi f_1 n} + e^{j(2\pi f_2 n + \theta)} + w(n) \tag{2.4}$$

where $f_1 = .115$, $f_2 = .135$, θ is random phase and w(n) is the white noise sequence.

The theoretical correlation matrix $\mathbf{R}$ is:

$$\mathbf{R}=\begin{bmatrix} 2+\sigma_w^2 & e^{-j2\pi 2_1}+e^{-j2\pi 2_2} & \cdots & e^{-j2\pi 2_1(M-1)}+e^{-j2\pi 2_2(M-1)} \\ e^{j2\pi 2_1}+e^{j2\pi 2_2} & 2+\sigma_w^2 & \cdots & e^{-j2\pi 2_1(M-2)}+e^{-j2\pi 2_2(M-2)} \\ \vdots & \vdots & \ddots & \vdots \\ e^{j2\pi 2_1(M-1)}+e^{j2\pi 2_2(M-1)} & e^{j2\pi 2_1(M-2)}+e^{j2\pi 2_2(M-2)} & \cdots & 2+\sigma_w^2 \end{bmatrix} \quad (2.5)$$

The estimated correlation matrix $\mathbf{\Phi}$ is computed from the following Equation.

$$\mathbf{\Phi} = \mathbf{A}^H\mathbf{A} \quad (2.6)$$

where $\mathbf{A}$ is the data matrix and matrix $\mathbf{A}^H$ is expressed as the following equation.

$$\mathbf{A}^H = \begin{bmatrix} u(M) & u(M+1) & \cdots & u(N) \\ u(M-1) & u(M) & \cdots & u(N-1) \\ \vdots & \vdots & \ddots & \vdots \\ u(1) & u(2) & \cdots & u(N-M+1) \end{bmatrix} \quad (2.7)$$

where M is the rank of matrix $\mathbf{A}$.

Figure 2.1 shows the spectrum plots of two sinusoids in white noise background. The signal to noise ratio (SNR) in this simulation is 10 dB. The blue curve is the spectrum by 256 point FFT method. Since there are only 32 data samples available, we padded an additional 224 zeros. This curve shows that the FFT method cannot resolve two closely frequency spaced signals. The green and red curves are the spectrum estimated by the MUSIC algorithm. The correlation matrix of the green curve is based on the theoretical equation defined by Equation (2.5); the correlation matrix of the red curve is a derivation based on the simulated data defined by Equation (2.6). Both curves show two clear peaks. The peaks of the green curve are at normalized frequencies of 0.1152 and 0.1348, respectively. They are very close to the true frequencies. The peaks of the red curve are at normalized frequencies of 0.1133 and 0.1387 respectively. They are a little bit off the true signal frequencies compared with the theoretical result. Also, their peaks are about 10 dB below the corresponding green curve. This Figure clearly shows that the MUSIC spectrum is very effective in resolving closely frequency spaced signals. A 5×5 matrix correlation matrix was used in this simulation study.

Figure 2.1 shows the performance degradation of the MUSIC algorithm based on finite received data samples. Increasing the sample number improves the estimation of correlation matrix and consequently an improved signal frequency estimation can be achieved. Figure 2.2 compares the performance of frequency estimation by the MUSIC algorithm with 32, 64 and 128 data samples. The red, green and blue curves in Figure 2.2 are MUSIC spectrum plots based on 32, 64 and 128 data samples. The peak frequencies are listed in Table 2.1. Table 2.1 and Figure 2.2 show that as the number of data sample increases, the estimated frequencies get closer to the true signal frequencies and the peaks of the MUSIC spectrum also increase.

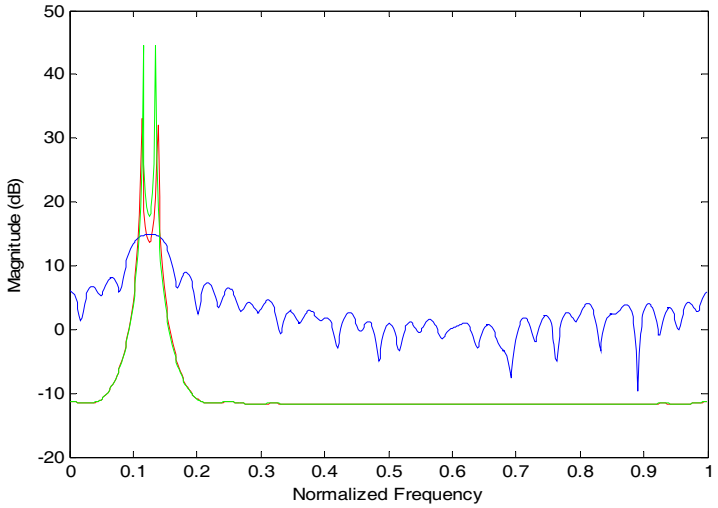

Fig. 2.1 Frequency Estimation by FFT and MUSIC Methods

	f_1	f_2
N = 32	0.1113	0.1387
N = 64	0.1152	0.1367
N=128	0.1152	0.1348

Table 2.1 Peak Frequencies of the MUSIC Spectrum

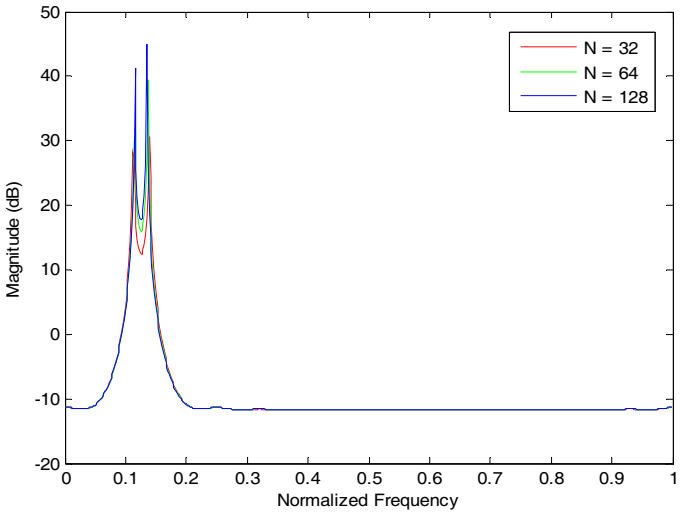

Fig. 2.2 Frequency Estimation by the MUSIC Method with 32, 64 and 128 Data Samples

Frequency estimation using the MUSIC algorithm can be considered as processing the received waveform in time domain (temporal) processing. This algorithm can also apply to spatial processing such as applications of sensor array systems.

Suppose there is a narrowband signal that impinges upon the uniformly spaced linear array antenna (ULA) with incident angle θ. The inter-element spacing of ULA d is d = λ/2, where λ is the signal wavelength. The ULA configuration is shown in Figure 2.3.

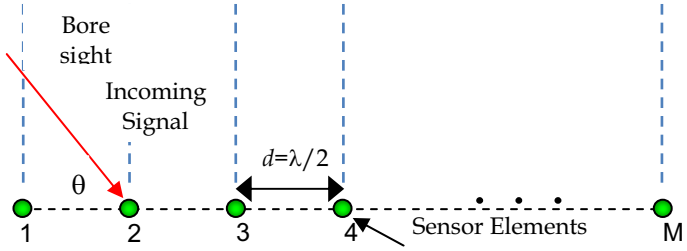

Fig. 2.3 Uniformly Spaced Linear Array Antenna

The narrowband waveform can be modeled as:

$$s(t) = m(t)\, e^{j2\pi f_c t} \tag{2.8}$$

where f_c is the center frequency.

If the signal impinges on the ULA with incident angle θ, the additional propagation path of the adjacent sensor is dcosθ. This additional path causes a propagation delay $\tau = d\cos\theta/c$ where c is the speed of light. If we choose the signal received by the first sensor $s_1(t)$ as the reference, the signal picked up by the k^{th} sensor $s_k(t)$ is

$$s_k(t) = m[t - (k-1)\tau]\, e^{j2\pi f_c (t-(k-1)\tau)} \tag{2.9}$$

From the narrowband signal assumption, $m(t - (k-1)\tau) \approx m(t)$, and defining the electrical angle β as $\beta = -2\pi d\cos\theta/\lambda$, signal $s_k(t)$ can be expressed as

$$s_k(t) = s_1(t) e^{j(k-1)\beta} \tag{2.10}$$

If there are L independent signals impinging on the ULA with incident angle $\theta_1, \ldots, \theta_L$, in the presence of independent white noise with variance σ_w^2, then the theoretical spatial correlation matrix **R** of the ULA is

$$\mathbf{R} = \mathbf{SPS}^H + \sigma_w^2 \mathbf{I} \tag{2.11}$$

where matrices **P** and **S** are defined by:

$$\mathbf{P} = \mathrm{diag}[P_1, \ldots, P_L] \tag{2.12}$$

$$\mathbf{S} = \begin{bmatrix} 1 & 1 & \cdots & 1 \\ e^{j\beta_1} & e^{j\beta_2} & \cdots & e^{j\beta_L} \\ \vdots & \vdots & \ddots & \vdots \\ e^{j(N-1)\beta_1} & e^{j(N-1)\beta_2} & \cdots & e^{j(N-1)\beta_L} \end{bmatrix} \tag{2.13}$$

and σ_w^2 is the noise variance, P_k, k = 1, 2, . . , L . are the power of k^{th} signal.

The estimated spatial covariance matrix $\mathbf{\Phi}$ using temporal average method with M snapshots is given as:

$$\mathbf{\Phi} = \mathbf{A}^H\mathbf{A} \tag{2.14}$$

where $\mathbf{A}$ is the data matrix, matrix $\mathbf{A}^H$ is given by the following equation.

$$\mathbf{A}^H = [\mathbf{u}_1, \mathbf{u}_2, \ldots, \mathbf{u}_N] \tag{2.15}$$

and $\mathbf{u}_k = [u_1(k), u_2(k), \ldots, u_M(k)]^T$ is the received data vector of sensor array or the snapshot at sample time k, N is the number of snapshot.

The estimated correlation matrix $\mathbf{\Phi}$ asymptotically approaches the theoretical matrix $\mathbf{R}$ as the number of snapshots increases. Therefore in order to have an accurate estimation of the correlation matrix the observation time must be sufficiently long. However, some real time radar signal processing applications cannot afford a long observation time. Correlation matrix estimation techniques like the spatial smoothing method (Haykin, 2002) are better suited for use in time sensitive systems.

Equations (2.2), (2.11) show that both temporal and spatial processing have an identical mathematical form. The following example shows the application of spectral processing to estimate the signal DOA using the MUSIC algorithm. The scan vector $\mathbf{s}$ used in this application is $\mathbf{s}(\theta) = [1, e^{j\beta}, \ldots, e^{j(M-1)\beta}]^T$, where parameter β is related to the DOA angle by $\beta = -2\pi d\cos\theta/\lambda$.

Suppose there are two narrowband signals impinging upon the 16 element ULA from angles of 40° and 50°. The estimated signal DOA can be found from the peak of the MUSIC spectrum. The SNR in this simulation is 10 dB and the estimated correlation matrix is based on simulated data averaged over 32 snapshots. Figure 2.4 shows the simulation result of the estimated DOA using a ULA consisting of 6, 8 and 10 elements.

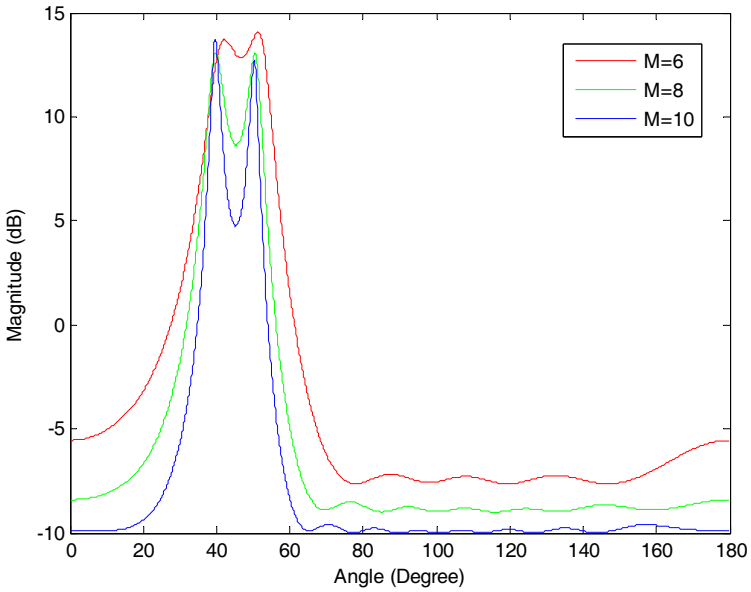

Fig. 2.4 DOA Estimation using ULA with 6, 8, 10 Elements

From Figure 2.4, with 6 element ULA (red curve), the MUSIC spectrum barely shows two peaks. As the number of elements increases to 8 (green curve) and 10 (blue curve), the MUSIC spectrum clearly shows two distinct peaks. The peak values of the green curve are at 39.6° and 50.1°, the peak values of the blue curve are at 39.8° and 50.3° respectively. The estimated DOA angles are fairly close to the true DOA angles.

Equation (2.14) shows the estimated correlation matrix based on temporal averaging over N snapshots. Increasing the number of snapshots N improves the estimation of the covariance matrix. Improving the estimation of the correlation matrix provides a more accurate DOA estimation. Figure 2.5 shows the DOA estimation using an 8 element ULA with an estimated covariance matrix based on temporal averaging over 16 (red curve), 32 (green curve) and 64 (blue curve) snapshots.

The peak values of the MUSIC spectrum in Figure 2.5 are listed in Table 2.2.

	θ_1	θ_2
N = 16	38.8°	50.8°
N = 32	39.6°	50.5°
N = 64	40.1°	49.9°

Table 2.2 Peak Values of the MUSIC Spectrum

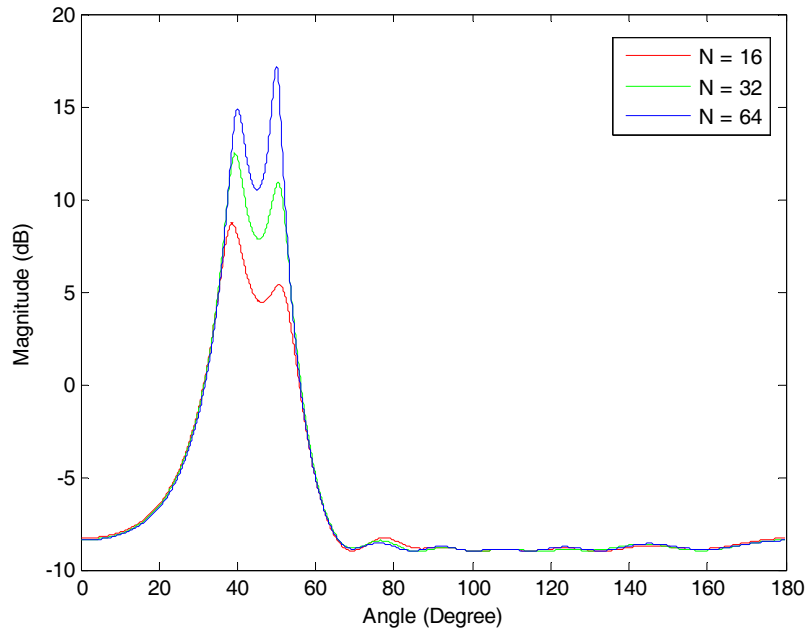

Fig. 2.5 DOA Estimation using an 8 Element ULA with Temporal Averaging over 16, 32, 64 Snapshots

Figure 2.5 and Table 2.2 show that the accuracy of the DOA estimation can be improved by increasing the number of snapshots in the correlation matrix estimation. Increasing the number of snapshots from 16 to 32 to 64 not only provides clearer peaks, but their peak values also increase.

3. Root Music Algorithm

To estimate frequency or signal DOA angles with the MUSIC algorithm requires using a scan vector to scan over all possible frequencies or over all possible direction angles. To obtain fine resolution, we need many frequency or angle sample points. Consequently, it requires high processing resources. Root MUSIC algorithm is a modification to MUSIC without using a scan vector. The estimated frequencies or DOA angles can be obtained by finding the L roots closest to unit circle of the following Equation.

$$J(z) = \mathbf{z}^H \mathbf{V}_N \mathbf{V}_N^H \mathbf{z} = 0 \tag{3.1}$$

where the steering vector $\mathbf{z}$ is

$$\mathbf{z} = [1, z^{-1}, z^{-2}, \ldots, z^{-(N-1)},]^T \tag{3.2}$$

and $z = e^{j2\pi f}$ for frequency estimation and $z = e^{j\beta}$ for angle estimation.

The frequency and angle are determined by the following Equations.

$$f_k = \frac{1}{2\pi}\arg(z_k) \quad , \quad k = 1, 2, \ldots, L \tag{3.3}$$

$$\theta_k = \cos^{-1}\left[\frac{\lambda}{2\pi d}\arg(z_k)\right], \quad k = 1, 2, \ldots, L \tag{3.4}$$

The roots of J(z) contain the directional information of the incoming signals. Ideally, the roots of J(z) corresponding to the signals' frequency or DOA would be on the unit circle, however due to the presence of noise the roots may not necessarily be exactly on the unit circle. In this case, the L roots closest to the unit circle represent the L incoming signals frequencies or DOA. These selected roots, by themselves, do not directly represent the frequency or incoming angle. For each root, the frequency or incoming angle can be found by computing Equations (3.3) and (3.4).

Consider a 16 elements ULA with an inter-element spacing that equals one half wavelength. If this were a conventional fixed antenna, its mainlobe beamwidth would be around 7°. This antenna array will not be able to resolve multiple signals if their angle separation is less than 7 degrees. Using the root MUSIC algorithm, this ambiguity can be easily resolved.

Let $x_i(1)$, $x_i(2)$, ... , $x_i(N)$ represent the received data samples from i^{th} element, where i = 1, 2, . . , M. The incoming data matrix **A** can be given

$$\mathbf{A}^H = \begin{bmatrix} x_1(1) & x_1(2) & .. & x_1(N) \\ x_2(1) & x_2(2) & .. & x_2(N) \\ : & : & :: & : \\ x_M(1) & x_M(2) & .. & x_M(N) \end{bmatrix} \tag{3.5}$$

The estimated correlation matrix $\mathbf{\Phi}$ is computer by

$$\mathbf{\Phi} = \mathbf{A}^H\mathbf{A} \tag{3.6}$$

From the estimated correlation matrix $\mathbf{\Phi}$, the eigenvalues can be computed. The columns of matrix $\mathbf{V}_N$ are the eigenvectors associated with the M-L smallest eigenvalues of matrix $\mathbf{\Phi}$. Once this matrix is available, the signals DOA can be derived from L roots of the polynomial J(z) closest to the unit circle.

If there are two signals impinging upon a 16 element ULA from angles of 40° and 46°, the roots computed from Equation (3.1) are shown in Figure 3.1. In this simulation, the number of snapshots N is 32 and the signal to noise ratio is 20 dB.

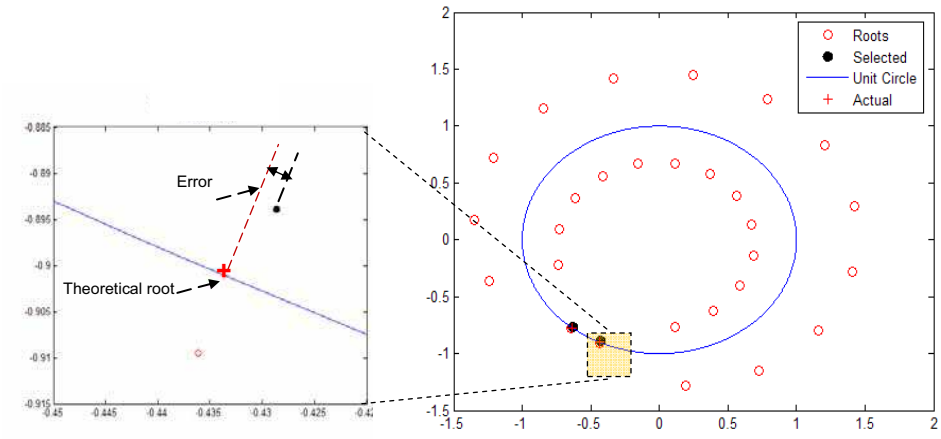

Fig. 3.1 Roots Polynomial J(z)

Figure 3.1 shows that when the angle separation between two signals is smaller than the mainlobe beamwidth, two distinct pairs of roots closest to the unit circle can easily be identified. It is shown in the zoom area that one of the roots is very close to the theoretical root of the signal DOA. Further reduce the angle separation to 3°, and 1.5°, and the results are very similar to Figure 3.1. Thus, the spatial resolution is improved by root MUSIC algorithm.

Equation (3.4) converts the roots of polynomial J(z) to the signal DOA. Assume there are two signals impinging on a 16 element ULA with 20 dB SNR and taking 32 snapshots, histograms of the estimated signal DOA with different angle separations are shown in Figure 3.2.

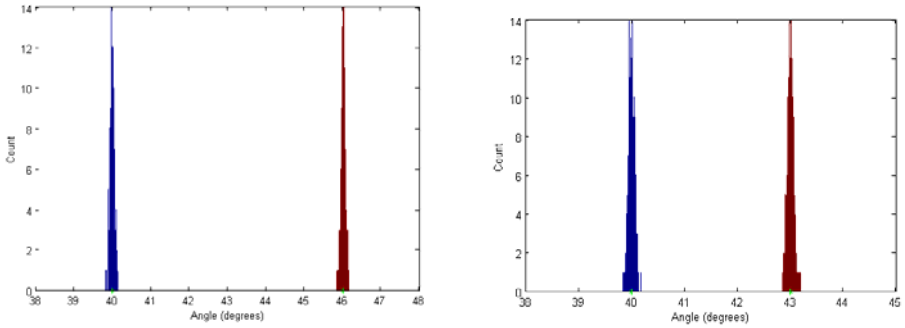

(a) (b)

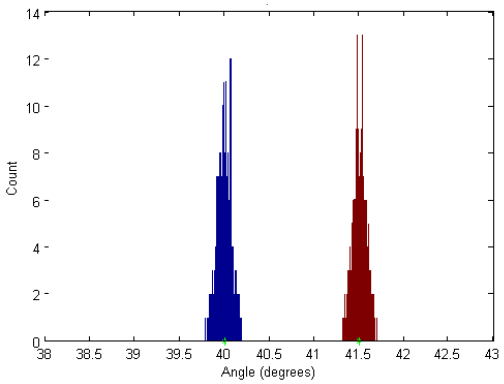

(c)

Fig. 3.2 Histograms of the Estimated Signal DOA for Angle Separation equal 6°, 3°, and 1.5°

The estimated means and variances based on 1000 trials are summarized in Table 3.1.

Angle Separation	6°	3°	1.5°
True Angles	40° 46°	40° 43°	40° 41.5°
Estimated Mean	39.9972° 46.0041°	39.9998° 42.9995°	39.9999° 41.4987°
Variance	0.0009 0.0012	0.0023 0.0025	0.0047 0.0042

Table 3.1 Estimated Mean and Variance of DOAs for SNR = 20 dB

Figure 3.2 and Table 3.1 show that the estimation variance increases as the angle separation becomes smaller.

Increasing the estimated correlation matrix from 32 snapshots to 96 snapshots reduces the estimated variance. Figure 3.3 compares the histogram of the estimated signals' DOA for 20 dB SNR, and the signals' DOA are 40° and 41.5° for 32 and 96 snapshots. The estimated mean values and variances based on 1000 trials are listed in Table 3.2.

Number of Snapshots	32	96
True Angles	40° 41.5°	40° 41.5°
Estimated Mean	39.9999° 41.4987°	39.9992° 41.5008°
Variance	0.0047 0.0042	0.0015 0.0016

Table 3.2 The Estimated Mean and Variance of DOAs for SNR = 20 dB

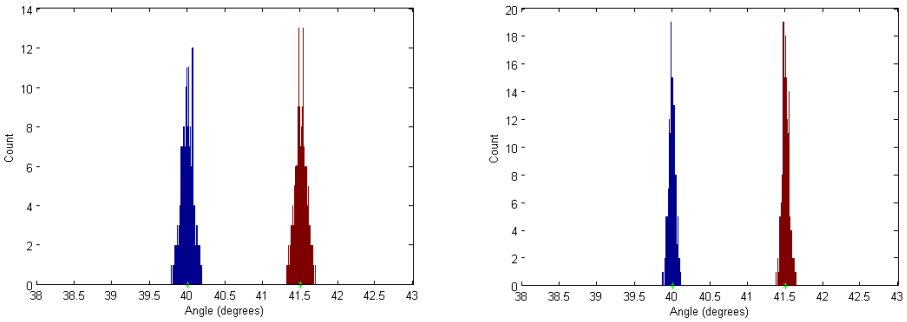

(a) (b)

Fig. 3.3 Histogram of the Estimated Signals' DOA with SNR = 20 dB and Signals' DOA are 40° and 41.5° (a) 32 Snapshots, (b) 96 Snapshots.

The above simulation results assume that the system operates in a high SNR environment. The SNR is 20 dB. If the SNR is only 5 dB, the simulation result yields a larger estimation variance. Figure 3.4 shows the histogram of the estimated signals' DOA for 5 dB SNR, and the signals' DOA are 40° and 46°. This result is based on 1000 independent simulations where the number of snapshots in each simulation is 32 and 96, respectively.

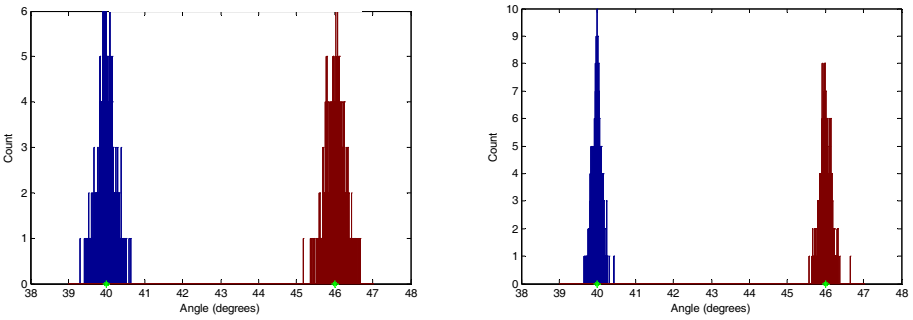

(a) (b)

Fig. 3.4 Histogram of the Estimated Signals' DOA with SNR = 5 dB, (a) 32 Snapshots (b) 96 Snapshots, Signals' DOA are 40° and 46°

The estimated mean values and variances based on 1000 trials for 5 dB SNR and the two different numbers of snapshots are listed in Table 3.3.

Number of Snapshots	32	96
True Angles	40° 46°	40° 46°
Estimated Mean	39.9708° 46.0279°	39.9893° 46.0094°
Variance	0.0358 0.0430	0.0112 0.0140

Table 3.3 The Estimated Mean and Variance of DOAs for SNR = 5 dB

This simulation result shows that increases in the number of snapshots provide a better correlation matrix estimation; consequently, the estimation variance decreases.

4. PRIME Algorithm

Root MUSIC can only estimate one DOA angle. A signal impinging on the array anywhere on the cone with its axis aligned with the array elements yields the identical result. This angle ambiguity is shown in Figure 4.1. This angle ambiguity can be resolved by using a two dimensional array. The PRIME algorithm is a method that allows polynomial rooting techniques to be applied to multidimensional estimation.

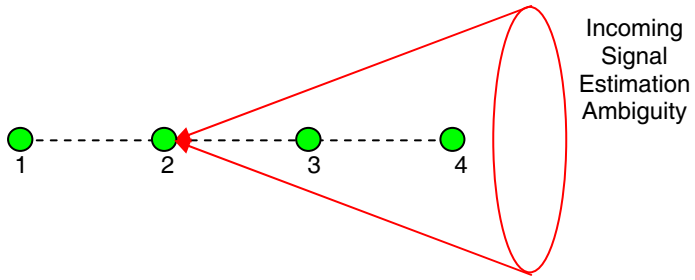

Fig. 4.1 Angle Ambiguity of ULA

Consider a general array of M sensors as shown in Figure 4.2. The coordinate of the i^{th} sensor is $\mathbf{r}_i = [x_i, y_i, z_i]^T$, i = 1, 2, … , M.

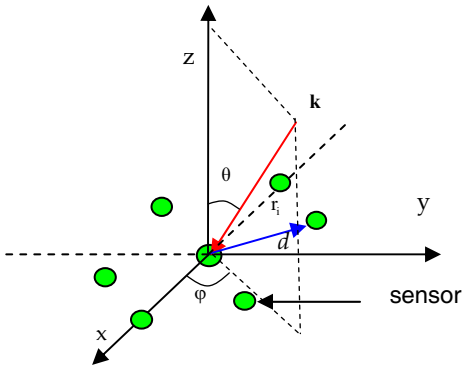

Fig. 4.2 An Array of M Sensors

Suppose a plane target signal waveform comes from the direction of $\mathbf{k}$ = [sinθcosφ, sinθsinφ, cosθ]^T, where θ is the elevation angle and φ is the azimuth angle. The difference of the propagation path of this wave between the origin and the i^{th} sensor Δd_i is

$$\Delta d_i = \mathbf{r}_i^T \mathbf{k} = \sin\theta\,(x_i\cos\varphi + y_i\sin\varphi) + z_i\cos\theta \qquad (4.1)$$

The corresponding propagation time delay τ_i is

$$\tau_i = \Delta d_i / c \tag{4.2}$$

where c is the speed of light.

To avoid the effect of grating lobes, the distance between the two neighbor sensors has to be no more than one half of the wavelength. If the reference sensor is located at the origin, and a waveform received by the reference sensor due to signal coming from direction of **k** is x(t), then the received waveform at i^{th} sensor is $x_i(t) = x(t-\tau_i)$.

As shown in Figure 4.2, the array elements are placed on x-y plane, the elevation angle θ and azimuth angle φ uniquely define the signal DOA. For a narrowband signal, if the j^{th} signal DOA is (θ_j, φ_j), the relative phase shift of k^{th} element due to the j^{th} signal is defined by the following Equation:

$$\beta_{k,j} = -\frac{2\pi}{\lambda}\sin\theta_j(x_k\cos\varphi_j + y_k\sin\varphi_j) \tag{4.3}$$

In Equation (4.3), each signal has two unknown parameters, elevation angle θ_j and azimuth angle φ_j, that need to be determined. Thus, to obtain the DOA angles, two independent polynomials must be constructed and solved. There are several different techniques to derive two independent polynomials.

The first approach constructs the two independent Equations from two distinct subsets. Two distinct null spaces matrices $\mathbf{V}_{1N}$ and $\mathbf{V}_{2N}$ can be derived from two different subsets. The two independent Equations are:

$$J_1(z, w) = \mathbf{a}^H(z,w)\mathbf{V}_{1N}\mathbf{V}_{1N}^H\mathbf{a}(z,w) \tag{4.4}$$

$$J_2(z, w) = \mathbf{b}^H(z,w)\mathbf{V}_{2N}\mathbf{V}_{2N}^H\mathbf{b}(z,w) \tag{4.5}$$

where variables $z = e^{j\frac{2\pi}{\lambda}x\sin\theta\cos\varphi}$, $w = e^{j\frac{2\pi}{\lambda}y\sin\theta\sin\varphi}$. Vectors **a** and **b** depend on the subset configurations. To guarantee the two Equations are independent, the two subsets cannot relate to each other by a linear shifting relation. There are many different ways to choose the distinct subsets. The accuracy of DOA estimation depends on the configuration of the subarrays.

The second approach constructs two independent equations by using the full array. The columns of matrices $\mathbf{V}_{1N}$ and $\mathbf{V}_{2N}$ are chosen from eigenvectors associates with M-L smallest eigenvalues of the correlation matrix. To guarantee two equations are independent, column vectors of matrices $\mathbf{V}_{1N}$ and $\mathbf{V}_{2N}$ cannot identical. Since the full array is used, the two polynomials are:

$$J_1(z, w) = \mathbf{a}^H(z,w)\mathbf{V}_{1N}\mathbf{V}_{1N}^H\mathbf{a}(z,w) \tag{4.6}$$

$$J_2(z, w) = \mathbf{a}^H(z,w)\mathbf{V}_{2N}\mathbf{V}_{2N}^H\mathbf{a}(z,w) \tag{4.7}$$

where vector **a** is the array manifold vector.

If the signal DOA is (θ, φ) and the estimated DOA is $(\hat{\theta}, \hat{\varphi})$, the estimated angle error α_e is given by the following equation.

$$\alpha_e = \cos^{-1}(\sin\theta\sin\hat{\theta}\cos\varphi\cos\hat{\varphi} + \sin\theta\sin\hat{\theta}\sin\varphi\sin\hat{\varphi} + \text{cosvcos}\hat{\theta}) \tag{4.8}$$

The estimated correlation matrix based on Equation (2.14) is different from theoretical equation (2.11). In theoretical equation, the signal and noise are assumed independent. However, the estimation based on finite number of data samples does not satisfy independent condition.

According to Equation (2.11) elements of correlation matrix contain no cross coupling terms between signal and noise. However, estimation the elements of correlation matrix based on finite received data samples contain cross couple terms. This cross couple terms degrade the estimation performance.

Suppose there is only one signal, the input waveform to the i^{th} array element at sample time n $u_i(n)$ is

$$u_i(n) = Ae^{j(2\pi f_c n+\beta_i)} + w_i(n) \tag{4.9}$$

where $w_i(n)$ is the white noise with variance σ_w^2 and β_i is the relative signal phase of the i^{th} element.

The element r_{ij} of the correlation matrix is

$$r_{ij} = \sum_{n=1}^{N} u_i(n)u_j^*(n) = \sum_{n=1}^{N}\left[Ae^{j(2\pi f_c n+\beta_i)} + w_i(n)\right]\left[Ae^{-j(2\pi f_c n+\beta_j)} + w_j^*(n)\right]$$

$$= NA^2e^{j(\beta_i-\beta_j)} + \sum_{n=1}^{N}Ae^{j(2\pi f_c n+\beta_i)}w_j^*(n) + \sum_{n=1}^{N}Ae^{-j(2\pi f_c n+\beta_j)}w_i(n) + N\sigma_w^2\delta_{ij} \tag{4.10}$$

The term $NA^2e^{j(\beta_i-\beta_j)}$ is the component of r_{ij} due to the signal, $N\sigma_w^2\delta_{ij}$ is the component of r_{ij} due to the noise. $\sum_{n-1}^{N} Ae^{j(2\pi f_c n+\beta_i)}w_j^*(n) + \sum_{n-1}^{N} Ae^{-j(2\pi f_c n+\beta_j)}w_i(n)$ is the cross coupling term between the signal and noise is which has zero mean and variance is $2NA^2\sigma_w^2$.

If there are two signals impinging on the array, the input waveform to the i^{th} array element $u_i(n)$ at sample time n is

$$u_i(n) = A_1e^{j(2\pi f_1 n+\beta_{i1})} + A_2e^{j(2\pi f_2 n+\theta+\beta_{i2})} + w_i(n) \tag{4.11}$$

where β_{i1} and β_{i2} are the corresponding electrical angles due to signal 1 and signal 2, f_1, f_2 are the frequencies of two signals, random phase θ represent the relative delay of two signals.

The element r_{ij} of the correlation matrix is

$$\begin{aligned}
r_{ij} &= \sum_{n=1}^{N} u_i(n)u_j^*(n) \\
&= \sum_{n=1}^{N}\left[A_1e^{j(2\pi f_1 n+\beta_{i1})} + A_2e^{j(2\pi f_2 n+\theta+\beta_{i2})} + w_i(n)\right]\left[A_1e^{-j(2\pi f_1 n+\beta_{j1})} + A_2e^{-j(2\pi f_2 n+\theta+\beta_{j2})} + w_j^*(n)\right] \\
&= NA_1^2e^{j(\beta_{i1}-\beta_{j1})} + NA_2^2e^{j(\beta_{i2}-\beta_{j2})} + N\sigma_w^2\delta_{ij} + A_1A_2e^{j(\beta_{i1}-\beta_{j2}-\theta)}\sum_{n=1}^{N}e^{j2\pi\Delta fn} + A_1A_2e^{j(\beta_{i2}-\beta_{j1}+\theta)}\sum_{n=1}^{N}e^{-j2\pi\Delta fn} \\
&\quad + \sum_{n=1}^{N}A_1e^{j(2\pi f_1 n+\beta_{i1})}w_j^*(n) + \sum_{n=1}^{N}A_2e^{j(2\pi f_1 n+\beta_{i2}+\theta)}w_j^*(n) + \sum_{n=1}^{N}A_1e^{-j(2\pi f_2 n+\beta_{j1})}w_i(n) \\
&\quad + \sum_{n=1}^{N}A_2e^{-j(2\pi f_2 n+\theta+\beta_{j2})}w_i(n)
\end{aligned} \tag{4.12}$$

Terms $NA_1^2e^{j(\beta_{i1}-\beta_{j1})}$, $NA_2^2e^{j(\beta_{i2}-\beta_{j2})}$, $N\sigma_w^2\delta_{ij}$ are the contribution of r_{ij} due to two signals and noise. $A_1A_2e^{j(\beta_{i1}-\beta_{j2}-\theta)}\sum_{n=1}^{N}e^{j2\pi\Delta fn}$, $A_1A_2e^{j(\beta_{i2}-\beta_{j1}+\theta)}\sum_{n=1}^{N}e^{-j2\pi\Delta fn}$ are the cross coupling term of two signals. If the frequency offset between two signals $\Delta f = f_1 - f_2$ is $\Delta f = k/N$ and k is an integer, those terms will be zero. The last four terms $\sum_{n=1}^{N}A_1e^{j(2\pi f_1 n+\beta_{i1})}w_j^*(n)$, $\sum_{n=1}^{N}A_2e^{j(2\pi f_1 n+\beta_{i2}+\theta)}w_j^*(n)$, $\sum_{n=1}^{N}A_1e^{-j(2\pi f_2 n+\beta_{j1})}w_i(n)$ and $\sum_{n=1}^{N}A_2e^{-j(2\pi f_2 n+\theta+\beta_{j2})}w_i(n)$ are the coupling between two signals and noise, their mean values are zero. If there are more than two signals, then there will be even more coupling terms which will further degrade the performance.